Published in Journal of Electroanalytical Chemistry 571, issue 1, 27-35, 2004
which should be used for any reference to this work

Current response of ion-selective solvent polymeric membranes at controlled potential

Jolanda Sutter [a], Werner E. Morf [b,*], Nicolaas F. de Rooij [b], Ernö Pretsch [a,*]

[a] *Laboratory for Organic Chemistry, Swiss Federal Institute of Technology, ETH Hönggerberg, CH-8093 Zürich, Switzerland*
[b] *Institute of Microtechnology (IMT), University of Neuchâtel, Rue Jaquet-Droz 1, CH-2007 Neuchâtel, Switzerland*

Abstract

From electrochemical measurements at the interface of two immiscible electrolytes, the current at controlled potential is usually a linear function of the ion concentration in the aqueous phase. Surprisingly, a linear relationship between the current and the logarithm of the sample ion activity is found for corresponding measurements on ion-selective electrode membranes. Here, a theoretical explanation for the apparent contradiction between the behavior of the two kinds of system is given. Experimental results obtained with conventional ion-selective PVC membranes as well as with membranes based on PVC free membrane matrices are presented.

Keywords: Ion-selective electrodes; Solvent polymeric membranes; Current response; Theory

1. Introduction

Ion-selective electrodes (ISEs) based on membranes with ionophores have gained a high relevance as analytical chemical tools [1–4]. In nearly all applications so far, they have been used as potentiometric sensors, i.e., for potential measurements at zero current. Nevertheless, experiments on ionophore membranes under the influence of an electrical current have a long tradition [5–7]. Such early investigations were often initiated to demonstrate the specific action of ionophores and to elucidate the response mechanisms of the respective membranes [8–10]. More recent experiments on ISE systems under current flow aimed at the optimization of response characteristics [11–13]. Actually, a current-induced modulation of the flux of primary ions through the membrane permits the improvement of the lower detection limit of a sensor by several orders of magnitude [11,12]. This effect is in close analogy to the behavior reported for conventional membrane ISEs where the zero-current counter transport of two ionic species can be suppressed to achieve lower detection limits down to 10^{-12} M in buffer-free samples [14,15]. Several investigations on ISE assemblies are based on pulsed or cyclic electrochemical measuring techniques and were meant to lead to new types of ion sensors [16–24]. A different group of fundamental studies focused on the electrochemistry at the interface between two immiscible electrolyte solutions (ITIES) [25–28] in place of the complete three-phase membrane arrangement [29] used in ISE cells.

Practical applications of ionophore membranes in a controlled-potential mode may have been impeded by the fact that the reported current response behavior of such systems seems to be quite contradictory. From pulsed or cyclic measurements on ion-selective PVC membranes, the current signals were claimed to be proportional to the logarithm of ion activity or concentration [8,9,20–24]. In contrast, from studies on ITIES using organic phases containing ionophores, the voltammetric or amperometric responses were apparently found to depend linearly on the ion concentration

* Corresponding authors. Tel.: +41-1-632-29-26; fax: +41-1-632-11-64.
E-mail address: pretsch@org.chem.ethz.ch (E. Pretsch).

[26–28,30]. Similarly, membranes without or with only a very low PVC content also showed a linear dependence of the signal on the sample ion activity [16,18,19].

Here, we report on new results on the current response of ionophore-based ISEs at controlled potential. A theoretical approach is presented to explain the puzzling electrochemical behavior of ISE membranes and related model systems.

2. Theory

Nearly all electrical aspects of ionophore-based cation-selective electrodes can be interpreted by a theoretical model that treats the membrane as an electrically neutral phase incorporating immobile anions ("fixed" sites) [5,13,31,32]. Together with the ionophores as ion-specific complex formers, the anionic sites ensure a highly selective transfer of primary cations into and through the membrane. The current flow within an ideally selective membrane is then found to follow the ohmic law [13,31]:

$$I = AFz_I J_I = -\frac{1}{R_m}\Delta\phi_m, \tag{1}$$

$$R_m = \frac{(RT/z_I F)d}{AFD_{I,m}c_{R,m}}, \tag{2}$$

where I is the electrical current, J_I the total flux of primary ions I^{z_I} of charge z_I (which exist predominantly as ionophore complexes in the membrane), $\Delta\phi_m$ the electrical potential drop within the membrane, R_m the inner membrane resistance, A the active membrane area, d the membrane thickness, $D_{I,m}$ the average diffusion coefficient of primary ions in the membrane, $c_{R,m}$ the given total concentration of anionic sites (assumed to be singly charged), F the Faraday constant, R the universal gas constant, and T the absolute temperature.

The transmembrane flux of primary ions is coupled with an equivalent diffusion flux through the Nernstian boundary layers of sample and the internal solutions, respectively. Hence, a current-induced difference arises between the nominal ion concentration, $c_{I,aq}$, in the bulk of the sample solution and its boundary concentration, $c'_{I,aq}$, next to the membrane surface (see Fig. 1):

$$I = I'_{lim}\frac{c_{I,aq} - c'_{I,aq}}{c_{I,aq}}, \tag{3}$$

$$I'_{lim} = \frac{AFz_I D_{I,aq}c_{I,aq}}{\delta}, \tag{4}$$

where I'_{lim} is the diffusion-limited current reached for $c'_{I,aq} \to 0$, $D_{I,aq}$ is the diffusion coefficient of the ions I^{z_I} in aqueous solutions, and δ the thickness of the aqueous boundary layer on the sample side. An analogous description holds for the other side of the membrane, accounting for a difference between the bulk concentration, $c^*_{I,aq}$, of the internal solution and the respective boundary concentration, $c''_{I,aq}$:

$$I = -I''_{lim}\frac{c^*_{I,aq} - c''_{I,aq}}{c^*_{I,aq}}, \tag{5}$$

$$I''_{lim} = \frac{AFz_I D_{I,aq}c^*_{I,aq}}{\delta^*}, \tag{6}$$

where I''_{lim} is the limiting current value defined for the inner diffusion layer of thickness δ^*. After replacing the concentration ratios in Eqs. (3) and (5) by the corresponding activity ratios, the boundary activities, $a'_{I,aq}$ and $a''_{I,aq}$, are readily expressed in terms of the respective bulk activities, $a_{I,aq}$ and $a^*_{I,aq}$

$$a'_{I,aq} = a_{I,aq}\frac{I'_{lim} - I}{I'_{lim}}, \tag{7a}$$

$$a''_{I,aq} = a^*_{I,aq}\frac{I''_{lim} + I}{I''_{lim}}. \tag{7b}$$

Another consequence of current flow in an ionophore membrane is that ion-bound ligands are translocated in the direction of the current, which leads to a concentration gradient of free ionophore L [5,6,31] (c.f., Fig. 1). At steady-state, conservation of the ionophore in the membrane requires that $J_L + n_I J_I = 0$, where J_L is the diffusion flux of uncomplexed ionophore, and J_I the

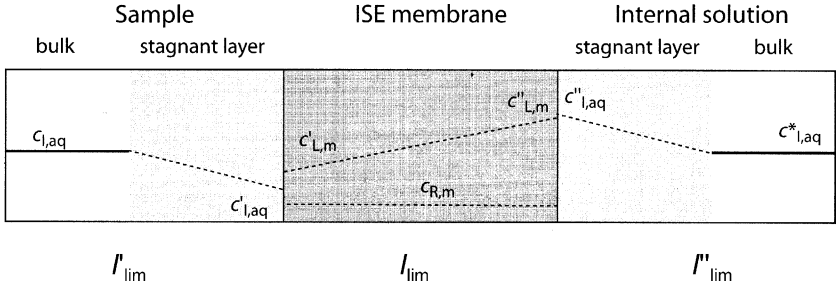

Fig. 1. Schematic representation of the applied model. The concentration profiles of primary ions, free ionophores (L), and anionic sites (R) are shown. The current can be limited by back-diffusion of free ionophores in the membrane (m) or by diffusion of the charge-carrying ions (I) in the stagnant layers of the two aqueous phases (aq). The presence of fixed sites is required for an equivalent amount of cationic ionophore complexes in the membrane and is decisive for the ohmic resistance at low currents.

current-induced flux of primary ions assumed to be transferred as ionophore complexes of a given 1:n_I stoichiometry. It follows [5,31] that:

$$I = -\frac{z_I}{n_I} AFJ_L = I_{lim}\frac{c''_{L,m} - c'_{L,m}}{2c_{L,m}}, \tag{8}$$

$$I_{lim} = \frac{2z_I}{n_I} AFD_{L,m}c_{L,m}/d, \tag{9}$$

where $c'_{L,m}$ and $c''_{L,m}$ are the boundary concentrations of free ionophores on the membrane surfaces contacting the sample and the internal solution, respectively, $c_{L,m} = 0.5 \times (c'_{L,m} + c''_{L,m})$ is the average concentration of uncomplexed ligands, $D_{L,m}$ the diffusion coefficient of the free ionophore, and I_{lim} a limiting current related to the maximum diffusion flux of ionophore within the membrane. Hence, we obtain

$$c'_{L,m} = c_{L,m}\frac{I_{lim} - I}{I_{lim}}, \tag{10a}$$

$$c''_{L,m} = c_{L,m}\frac{I_{lim} + I}{I_{lim}}. \tag{10b}$$

The boundary values specified in Eqs. (7) and (10) as well as the concentration of anionic sites are decisive for the distribution of exchangeable primary ions at the two membrane/solution interfaces. These quantities enter into the description of the two interfacial Galvani potential differences, $\Delta\phi'_b$ and $\Delta\phi''_b$ [5,13,31,32]:

$$\Delta\phi'_b = \frac{RT}{z_I F}\ln\left[z_I K'_I a'_{I,aq}/c_{R,m}\right] \quad \text{with} \quad K'_I = k_I\beta_{I,n}\left(c'_{L,m}\right)^{n_I}, \tag{11}$$

$$\Delta\phi''_b = \frac{RT}{z_I F}\ln\left[z_I K''_I a''_{I,aq}/c_{R,m}\right] \quad \text{with} \quad K''_I = k_I\beta_{I,n}\left(c''_{L,m}\right)^{n_I}, \tag{12}$$

where K'_I and K''_I are the overall distribution coefficients of primary ions, which are related to the standard Gibbs energy of ion transfer at the respective interfaces and include the influence of ion complexation in the membrane, k_I is the distribution coefficient of free primary ions, and $\beta_{I,n}$ the stability constant of the predominant 1:n_I ion–ionophore complexes. After substituting the boundary values in Eqs. (11) and (12) and recalling Eq. (1), we obtain the final result for the total membrane potential:

$$E = \Delta\phi_m + \Delta\phi'_b - \Delta\phi''_b, \tag{13}$$

$$E = \frac{RT}{z_I F}\ln\left[a_{I,aq}/a^*_{I,aq}\right] - R_m I + \frac{RT}{z_I F}\ln\frac{1 - I/I'_{lim}}{1 + I/I''_{lim}} + \frac{n_I RT}{z_I F}\ln\frac{1 - I/I_{lim}}{1 + I/I_{lim}}, \tag{14}$$

where E is the potential difference between the bulks of the internal and sample solutions and I is the current flowing from the sample to the internal solution. In Eq. (14), the first term is the expression for the zero-current membrane potential, the second term is characteristic of an ohmic resistor, and the last two terms are in analogy to formal descriptions of polarographic waves accounting for the influences of current-induced concentration polarization in the aqueous phases and the membrane phase, respectively. It becomes evident that the current–voltage-activity behavior of ionophore membranes may be widely different depending on the various experimental parameters of the systems.

The preceding result indicates that the current response I obtained in experiments at constant potential is generally a function of the sample activity, $a_{I,aq}$. This becomes more obvious when Eq. (14) is rearranged

$$\frac{I}{I_o} - \ln\frac{1 - I/I'_{lim}}{1 - I/I''_{lim}} - n_I\ln\frac{1 - I/I_{lim}}{1 + I/I_{lim}} = \ln\frac{a_{I,aq}}{a^*_{I,aq}} - \frac{z_I F}{RT}E \tag{15}$$

with

$$I_o = \frac{RT}{z_I F}\frac{1}{R_m} = \frac{AFD_{I,m}c_{R,m}}{d}, \tag{16}$$

where I_o is a unit current corresponding to the current established for $\Delta\phi_m = -25.7$ mV/z_I at 25 °C. The exact type of the activity dependence in Eq. (15) is evidently dictated by the magnitude of the current relative to the parameters I_o, I'_{lim}, I''_{lim}, and I_{lim}.

The practical relevance of ISEs as amperometric sensors apparently hinges on the requirement that the parameter I_o is kept constant during the experiments, which implies that R_m must be sample-independent and invariant. This is not the case for thin membranes [33] but for the ISEs studied in this work it was found in hundreds of consecutive measurements [34] that the membrane resistance did not change significantly and can really be considered as a phenomenological constant.

The general result in Eq. (15) can also be considered as an extended description of ITIES systems. In typical ITIES experiments, however, limitations by ion transfer at an inner boundary, by free ionophore transport, as well as by the ohmic resistance are either nonexistent or largely excluded. For ISE systems, on the other hand, all these limiting terms may play a substantial role, depending on the magnitude of the various experimental parameters (see below).

3. Experimental

3.1. Reagents

Celgard® 2500 microporous flat sheet polypropylene membranes of 0.057×0.22 μm^2 pore size, 25 μm thickness, and 55% porosity were purchased from Celgard Inc. (Charlotte, North Carolina, USA). Poretics® polycarbonate membranes without wetting agent

(PVPF, poly(vinylpyrrolidone) free) of 14 μm pore diameter and 6 μm thickness were purchased from Osmonics Inc. (Minnetonka, Minnesota, USA). Poly(vinyl chloride) (PVC), the calcium ionophore *N, N*-dicyclohexyl-*N',N'*-dioctadecyl-3-oxapentanediamide (ETH 5234), potassium tetrakis-[3,5-bis-(trifluoromethyl)phenyl] borate (KTFPB), and tetrahydrofuran (THF) were Fluka Selectophore® and 2-nitrophenyl octyl ether (*o*-NPOE) puriss., p.a. from Fluka AG (CH-8701 Buchs, Switzerland). Aqueous solutions were prepared with freshly deionized water (18.0 MΩ cm specific resistance) obtained with a NANOpure™ reagent-grade water system (Barnstead, CH-4009 Basel, Switzerland); $CaCl_2$, NaCl, and KCl were Suprapur® from Merck (Darmstadt, Germany).

3.2. Membranes

Celgard®-based membranes contained ETH 5234 (2.3 wt%, 28.6 mmol kg^{-1}), KTFPB (0.3 wt%, 2.9 mmol kg^{-1}), and *o*-NPOE (97.4 wt%). A total of 270.4 mg of these components was dissolved in THF (2 ml) and a Celgard® membrane disk of 20 mm diameter was impregnated with 40 μl of the cocktail. The membrane was then immediately mounted in a symmetrical plexiglass cell allowing an exposed area of 0.64 cm^2 and with compartments of 20 ml on each side. Before starting emf/potential current measurements, the membrane was symmetrically conditioned in a 10^{-3} M $CaCl_2$, 10^{-3} M KCl, 10^{-4} M HCl solution for ca. 30 min.

Polycarbonate-based membranes contained ETH 5234 (2.4 wt%, 30.2 mmol kg^{-1}), KTFPB (0.3 wt%, 3.2 mmol kg^{-1}), and *o*-NPOE (97.3 wt%). A total of 272.4 mg of these components was dissolved in THF (2 ml). The THF was evaporated under air before a polycarbonate membrane disk of 20 mm diameter was impregnated with 2 μl of the cocktail. The membrane was then immediately mounted in the symmetrical plexiglass cell and conditioned for ca. 30 min as described above for the Celgard® membranes.

The PVC-based membranes contained ETH 5234 (1.6 wt%, 20.1 mmol kg^{-1}), KTFPB (0.2 wt%, 2.2 mmol kg^{-1}), *o*-NPOE (65.5 wt%), and PVC (32.7 wt%). Membranes of ca. 120 μm thickness were obtained by casting a solution of 404.4 mg of the membrane components dissolved in THF (ca. 4 ml) into a glass ring (44 mm i.d.) fixed on a glass plate. The PVC membranes were mounted in the symmetrical plexiglass cell and conditioned as described above but for 48 h.

3.3. Emf measurements

Potentials were measured with a custom-made 16-channel electrode monitor in the symmetrical plexiglass cell, both compartments of which were stirred. Two identical reference electrodes (Metrohm type 6.0726.100, Ag | AgCl in 3 M KCl, Metrohm AG, CH-9101 Herisau, Switzerland) with a bridge electrolyte of 1 M KCl were used as reference and working electrodes.

3.4. Controlled potential measurements

Current measurements at controlled potential were performed on all ISE membranes with the same symmetrical cell as described above. For these measurements a four electrode setup was used. The cell was equipped with working and counter electrodes Ag | AgCl (0.64 cm^2) and two identical reference electrodes as mentioned under 3.3 with a bridge electrolyte of 1 M KCl. The external potential difference was controlled with an SI 1287 Electrochemical Interface (Solartron Instruments, Farnborough, Hampshire, UK) using CorrWare software (Scribner Associates, Inc., Southern Pines, NC, USA). The same instrument was used to measure the current response. For each concentration, current readings were taken after 30 min. In order to guarantee a direct and true comparison between potentiometric and amperometric ISE responses, one and the same experimental set-up was applied for all measurements in this work. The membrane electrode cell basically conforms to the arrangement used for most practical ISE applications. It should be mentioned, however, that more sophisticated approaches to amperometric measurements with compensation of the ohmic potential drop have been introduced and described earlier (see, e.g. [10,35,36]).

4. Results and discussion

In the theoretical section, it was shown that three diffusion processes may limit the current measured on ISE membranes at controlled potential. The diffusion-controlled limiting currents in the two aqueous phases are related to the respective maximum values of the ionic concentration gradients, while the maximum migration current through the membrane is determined by the back-diffusion process of the free ionophores (see Fig. 1). In the case of plasticized polymer membranes used for conventional ISEs, the diffusion coefficient of primary ions in the membrane phase is lower than in aqueous solutions by at least two orders of magnitude [37–40]. Thus, the membrane resistance is high and the value of I_o comparatively low. It follows that $I_o \ll I'_{lim}$ and $I_o \ll I''_{lim}$ hold as long as both aqueous solutions contain adequate concentrations of primary ions (cf. Eqs (4), (6) and (16)). If the membrane contains an excess of free ionophores, i.e., $c_{L,m} \gg c_{R,m}$, the condition $I_o \ll I_{lim}$ is also fulfilled (cf. Eqs. (9) and (16)). Accordingly, the last two terms on the left of Eq. (15) can be neglected except for extremely high values of the applied voltage, and the current response reduces to the simple Eq. (17)

$$I = \frac{RT}{z_I F R_m} \ln \frac{a_{I,aq}}{a^*_{I,aq}} - \frac{E}{R_m} = \text{const} + \frac{RT}{z_I F R_m} \ln a_{I,aq}. \qquad (17)$$

An ISE membrane system of this type evidently behaves as an ohmic resistor that yields a current response to the actual overpotential, i.e., to the applied potential difference minus the zero-current membrane potential. Hence, the current signal is a linear function of the logarithm of the sample ion activity, the intercept being constant if the composition of the internal solution and the applied potential are constant. It should be noted that Eq. (17) can be derived immediately from the Nernstian zero-current potential plus the ohmic potential drop (Eq. (14) without the last two terms). Since this description is obviously restricted to special cases or limited ranges, however, the full theory has to be applied for an adequate analysis of the complete current response curve.

Contrasting response behavior is expected for ISE membranes that basically consist of a nonpolymeric solvent phase with a relatively high concentration of dissolved electrolyte. Since the diffusion coefficients in a liquid phase of low viscosity are much higher, the conditions $I'_{lim} \ll I_o$ and $I'_{lim} \ll I_{lim}$ may hold. In this case, the sample concentration must be fairly low, which also guarantees that $I'_{lim} \ll I''_{lim}$. Finally, the second term on the left of Eq. (15) becomes decisive, leading to

$$I = I'_{lim}\left[1 - e^{z_I FE/RT} \frac{a^*_{I,aq}}{a_{I,aq}}\right] = \frac{AFz_I D_{I,aq} c_{I,aq}}{\delta} \quad (\text{for } z_I E \to -\infty). \qquad (18)$$

Such systems behave in analogy to amperometric or voltammetric electrodes. They reflect the characteristics of ion transfer across the interface between two immiscible electrolyte solutions [25–28]. Accordingly, at sufficiently high voltages, a diffusion-limited current is reached that is directly proportional to the sample ion concentration.

An intermediate case is encountered for polymeric ISE membranes at very low sample activities. Here, the conditions $I_o \ll I''_{lim}$ and $I_o \ll I_{lim}$ still hold but also $I_o \approx I'_{lim}$. Therefore, the first two terms on the left of Eq. (15) must be considered, which finally yields the following result:

$$I = \frac{RT}{z_I F R_m} \ln\left[\frac{a_{I,aq}(1 - I/I'_{lim})}{a^*_{I,aq}}\right] - \frac{E}{R_m} = \text{const} + \frac{RT}{z_I F R_m} \ln\left[a_{I,aq} + \Delta a_{I,el}\right] \qquad (19)$$

with

$$\Delta a_{I,el} = -I \frac{a_{I,aq}}{I'_{lim}} = -\frac{I \delta \gamma_{I,aq}}{AFz_I D_{I,aq}}. \qquad (20)$$

In comparison with Eq. (17), the modified response function in Eq. (19) contains an additional activity increment, $\Delta a_{I,el}$, which correspond to the electrical contribution to the lower detection limit [13]. As shown in Eq. (20), this term is directly related to the current density, I/A, through the membrane but is independent of other membrane parameters ($\gamma_{I,aq}$ is the activity coefficient of the primary ion in the sample). These equations demonstrate that the useful current-response range of ISE membranes at constant potential differs from the analytical range of the corresponding potentiometric sensors. The observed effects depend on the sign and the magnitude of the current signal established near the lower detection limit (see also the preliminary results given in [41]).

Theoretical current responses to the sample Ca^{2+} concentrations calculated from the general Eq. (15) are shown in Fig. 2. The diffusion coefficients used for

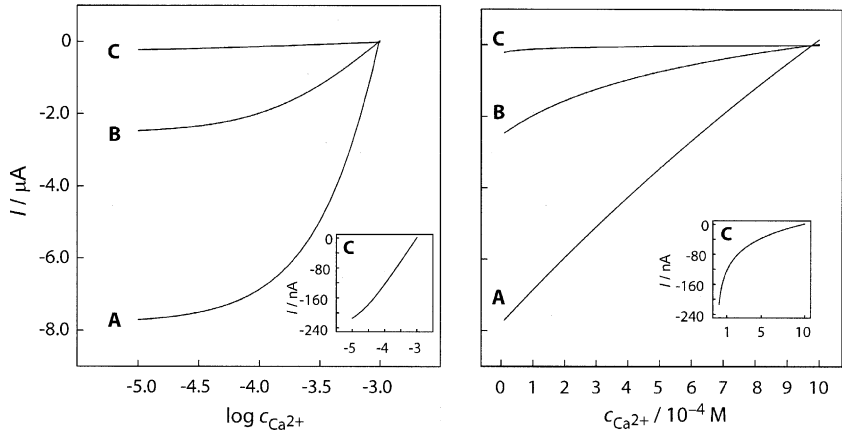

Fig. 2. Current response to the sample concentration, I vs. $\log c_{Ca^{2+}}$ (left) and I vs. $c_{Ca^{2+}}$ (right) calculated for an external potential of $E = -0.3$ mV applied to a membrane with an area of $A = 0.64$ cm^2. The thickness of the stagnant layer in the sample and internal solution was $\delta = \delta^* = 500$ µm, the internal solution had a Ca^{2+} concentration of 10^{-3} M, and the diffusion coefficient $D_{Ca,aq}$ was 7.92×10^{-6} cm^2 s^{-1} [45]. Curve A: membrane thickness $d = 20$ µm, $D_{I,m} = D_{L,m} = 5 \times 10^{-7}$ cm^2 s^{-1} ($R_M = 0.42$ kΩ). Curve B: membrane thickness $d = 60$ µm, $D_{I,m} = D_{L,m} = 10^{-7}$ cm^2 s^{-1} ($R_M = 6.24$ kΩ). Curve C: membrane thickness $d = 120$ µm, $D_{I,m} = 6 \times 10^{-9}$ cm^2 s^{-1}, $D_{L,m} = 3 \times 10^{-8}$ cm^2 s^{-1} ($R_M = 210.0$ kΩ).

curves A mimic the situation encountered with ITIES systems. Indeed, the response is almost linear if the current is plotted against the concentration (right side) but curved if it is shown as a function of the logarithmic concentration (left side). The opposite behavior is illustrated by curves C, which are based on experimentally obtained parameters for a plasticized Ca^{2+}-selective PVC membrane (see below). Here, the response to the logarithmic Ca^{2+} concentrations is practically linear and the response to the linear concentration scale is curved (see insert with 100 times enlarged scale of the *y*-axis). An intermediate case is shown by curves B, which were calculated with parameters obtained in this work for PVC-free ISE membranes (see below).

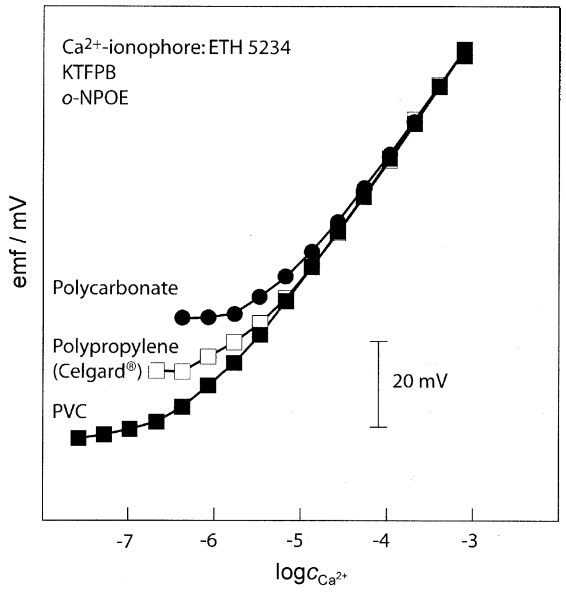

Fig. 3. Potentiometric response of a PVC-supported and two PVC-free Ca^{2+}-ISE membranes, the latter being based on microporous polypropylene (Celgard®) and track-etched polycarbonate as matrices. Internal solution: 10^{-3} M $CaCl_2$ with 10^{-3} M KCl and 10^{-4} M HCl, sample background: 10^{-3} M KCl and 10^{-4} M HCl. For better comparison, the curves were shifted to show the same emf at a sample concentration of 10^{-3} M.

Two kinds of PVC-free ISE membranes were investigated in this work in addition to the conventional PVC membrane. The first one was based on a matrix consisting of a microporous polypropylene (Celgard® 2500, 25 μm thickness). The elliptical pores (0.057×0.22 μm^2 pore size) formed by extrusion, annealing, and stretching were shown to be oriented with their major axes parallel to the film surface [42]. It has also been reported that a thin surface layer has a slightly smaller pore size and a lower two-dimensional pore area than the interior [42]. The other matrix consisted of track-etched Poretics® polycarbonate membranes having a thickness of 6 μm and pore diameters of 14 μm. The ISE membranes were obtained by impregnating these matrices with a solution of the ISE components (ionophore and ionic sites, see Section 3) in *o*-NPOE, which was also used as the plasticizer in the corresponding PVC membranes. First, the response of the three types of membranes was investigated in a conventional potentiometric setup (Fig. 3) using 10^{-3} M $CaCl_2$ with 10^{-3} M KCl and 10^{-4} M HCl as the internal solution. Due to the coextraction of a small amount of $CaCl_2$ from the internal solution into the membrane, zero-current transmembrane ion fluxes are known to influence the lower detection limit of such ISEs, which therefore shifts to higher values with increasing diffusion coefficients in, and decreasing thickness of, the membrane phase [32,43,44]. Indeed, the PVC membrane shows the most favorable lower detection limit (lowest ion fluxes) whereas the PVC-free membranes based on microporous polypropylene or polycarbonate matrices turn out to be worse by ca. half

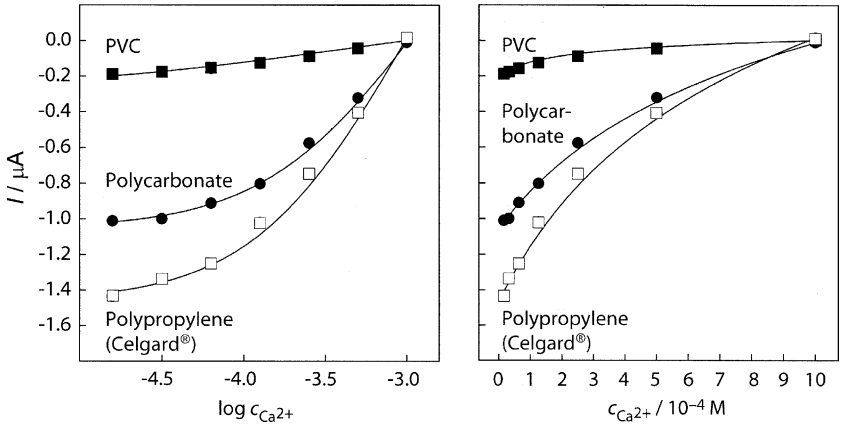

Fig. 4. Current response at constant external potential ($E = -0.3$ mV) of a PVC-supported and two PVC-free Ca^{2+}-ISE membranes (for details, see Fig. 3). Curves calculated from Eq. (15) with the following parameters: PVC membrane: $d = 120$ μm, $A = 0.64$ cm^2, $D_{I,m} = 6 \times 10^{-9}$ cm^2 s^{-1}, $D_{L,m} = 3 \times 10^{-8}$ cm^2 s^{-1} ($R_M = 212.0$ kΩ); polycarbonate membrane: $d = 42$ μm, $A = 0.23$ cm^2, $D_{I,m} = D_{L,m} = 9 \times 10^{-8}$ cm^2 s^{-1} ($R_M = 13.8$ kΩ); microporous polypropylene (Celgard®) membrane: $d = 58$ μm, $A = 0.35$ cm^2, $D_{I,m} = D_{L,m} = 1.05 \times 10^{-7}$ cm^2 s^{-1} ($R_M = 10.5$ kΩ). The thickness of the stagnant layer in the sample and internal solution was $\delta = \delta^* = 500$ μm in all cases.

and one order of magnitude, respectively (Fig. 3). Based on these results, it is expected that the amperometric response of the PVC-free membranes may differ from those of PVC membranes and will approach the behavior of the ITIES systems.

The current response of the three kinds of ISE membranes at a constant potential of $E = -0.3$ mV is shown in Fig. 4 together with the theoretical response curves (drawn lines) calculated from Eq. (15) with the parameters listed in the figure caption. On the logarithmic concentration scale (Fig. 4, left), the PVC membrane shows a perfectly linear current response as reported earlier [41]. In contrast, curved responses are obtained for the PVC-free polycarbonate and polypropylene membranes, respectively. As shown in Fig. 4, right, the response behavior of the latter two membrane systems is also curved if plotted as a function of concentration instead of the logarithmic plots. The fitted responses show that the membrane resistance (212.0 kΩ for the PVC membrane) is lowered to 13.8 and 10.5 kΩ when using PVC-free polycarbonate and polypropylene (Celgard®) membranes, respectively. The calculated response of the Celgard® membrane is based on the same diffusion coefficients as for curves B in Fig. 2. The reversed order of the potentiometric (Fig. 3) and current responses (Fig. 4) of the two PVC-free membranes can be explained by the fact that the limiting diffusion processes are not the same in the two cases. The heterogeneous structure of Celgard® (see above) apparently favors the back-diffusion of the free ligands that partly determines the limiting current in amperometric experiments.

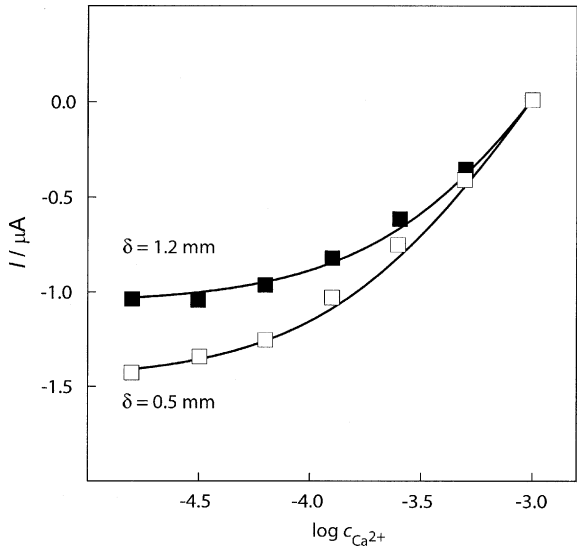

Fig. 5. Current response at constant external potential ($E = -0.3$ mV) of a Ca^{2+}-ISE membrane based on a microporous polypropylene (Celgard®) matrix (for details see Fig. 3). The thickness of the stagnant layer was increased in one experiment by placing an inert perforated polycarbonate membrane in front of the ISE membrane. The calculated curves are based on the same parameters as for Fig. 4 except for the thickness of the stagnant layer indicated in the figure.

Since various parameter combinations for the membrane phase may result in similar response curves, further experiments were carried out with Celgard® membranes, for which the current limitation by the ion transport in the membrane is relatively small. In one set of experiments (Fig. 5) the effective thickness of the unstirred layer was varied by fixing an inert hydrophilic polycarbonate membrane with holes of about 1 mm diameter (ca. 40 holes/cm^2) in the sample compartment of the cell, about 3 mm apart from the membrane surface. The two calculated amperometric response curves were based on the same parameters, except for the apparent thickness of the stagnant layer. Based on the very same set of parameters, it is also possible to describe the current responses at three applied potentials ($E = -0.3$, -30.0, and $+30.0$ mV, see Fig. 6). These results clearly indicate that the quantitative model according to Eq. (15) is sound and can be applied to various experimental setups.

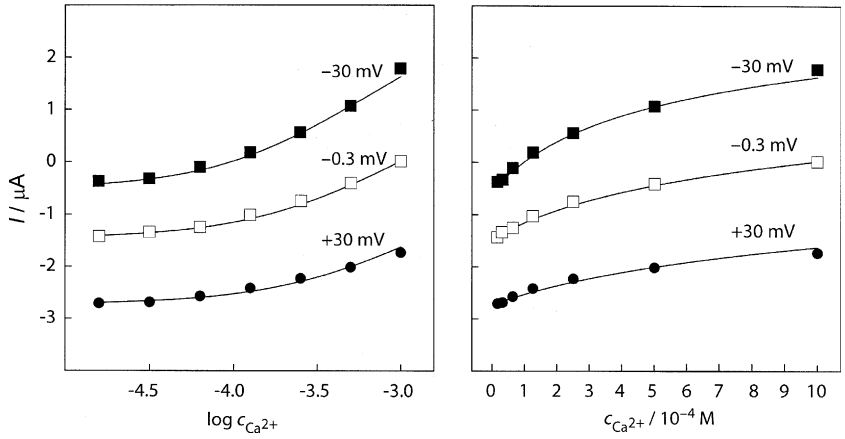

Fig. 6. Current response at different external potentials ($E = -0.3$, -30.0, or $+30.0$ mV) of a Ca^{2+}-ISE membrane based on a microporous polypropylene (Celgard®) matrix (for details see Fig. 3). The curves are calculated from Eq. (17) using the same parameters as in Fig. 4.

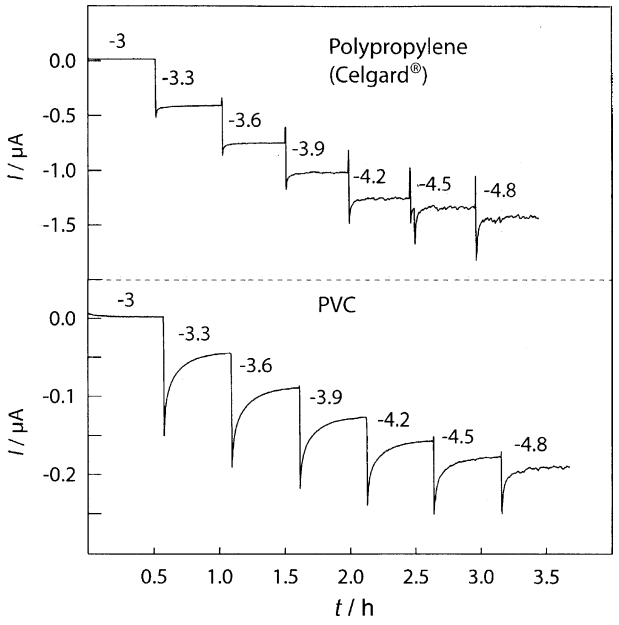

Fig. 7. Time traces of the current response at $E = -0.3$ mV of a PVC-supported and a PVC-free Ca^{2+}-ISE membrane, the latter being based on a microporous polypropylene (Celgard®) matrix (for details, see Fig. 3). The values given above the curves indicate the respective logarithmic molar Ca^{2+} concentrations in the sample.

All measurements discussed so far were based on steady-state current values. Depending on the type of membrane, this steady-state was achieved after different equilibration times. As shown by the time traces in Fig. 7, the Celgard® membranes exhibit fast responses and the respective steady states are reached within a few minutes. As expected, PVC-based membranes are much slower and the steady-state current value is achieved only about 0.5 h after the sample changes. Due to their fast response behavior, the Celgard® membranes are highly attractive candidates whenever fast transmembrane processes are required for potentiometric or amperometric sensing with liquid membrane electrodes.

5. Conclusions

The current response of ISE membrane assemblies at controlled potential was treated on a theoretical basis and studied in a series of experiments. The apparently contradictory amperometric response behavior obtained with ITIES and ion-selective PVC membranes was shown to originate from different kinetic limitations. For PVC-free liquid membranes based on inert microporous matrices, the response is neither a linear function when plotted vs. the logarithmic concentration, nor a linear function of the concentration itself. Hence, the behavior of these membranes is intermediate between that of PVC membranes and ITIES systems. Although potentiometric measurements with ISEs are still widely preferred for the determination of ion concentrations, the new amperometric method was shown to be an equivalent choice and may also find future applications in routine analysis.

Acknowledgements

The authors thank the Swiss National Science Foundation and the National Institutes of Health (grant 8R01EB002189-04) for financial support. We thank Dr. M. Badertscher for his help with the calculations and Dr. D. Wegmann for careful reading of the manuscript.

References

[1] J. Koryta, K. Stulik, Ion-Selective Electrodes, Cambridge University Press, Cambridge GB, 1983.
[2] E. Bakker, P. Bühlmann, E. Pretsch, Chem. Rev. 97 (1997) 3083.
[3] P. Bühlmann, E. Pretsch, E. Bakker, Chem. Rev. 98 (1998) 1593.
[4] E. Bakker, P. Bühlmann, E. Pretsch, Electroanalysis 11 (1999) 915.
[5] W.E. Morf, P. Wuhrmann, W. Simon, Anal. Chem. 48 (1976) 1031.
[6] A.P. Thoma, A. Viviani-Nauer, S. Arvanitis, W.E. Morf, W. Simon, Anal. Chem. 49 (1977) 1567.
[7] W.E. Morf, L.F.J. Dürselen, W. Simon, in: E. Roth (Ed.), Les éditions de physique, Les Ulis Cedex, Paris, 1988, p. 271.
[8] V. Horváth, G. Horvai, E. Pungor, Mikrochim. Acta 1990 (I) (1990) 217.
[9] G. Horvai, E. Pungor, Anal. Chim. Acta 243 (1991) 55.
[10] V. Horváth, G. Horvai, Anal. Chem. Acta 273 (1993) 145.
[11] E. Lindner, R.E. Gyurcsányi, R.P. Buck, Electroanalysis 11 (1999) 695.
[12] E. Pergel, R.E. Gyurcsányi, K. Tóth, E. Lindner, Anal. Chem. 73 (2001) 4249.
[13] W.E. Morf, M. Badertscher, T. Zwickl, N.F. de Rooij, E. Pretsch, J. Electroanal. Chem. 526 (2002) 19.
[14] T. Sokalski, A. Ceresa, T. Zwickl, E. Pretsch, J. Am. Chem. Soc. 119 (1997) 11347.
[15] E. Bakker, E. Pretsch, Anal. Chem. 74 (2002) 420A.
[16] K. Cammann, B. Ahlers, D. Henn, C. Dumschat, A.A. Shul'ga, Sens. Actuat. B 35 (1996) 26.
[17] H.J. Lee, P.D. Beattie, B.J. Murray, D. Osborne, H.H. Girault, J. Electroanal. Chem. 440 (1997) 73.
[18] H.J. Lee, H.H. Girault, Anal. Chem. 70 (1998) 4280.
[19] S. Sawada, H. Torii, T. Osakai, T. Kimoto, Anal. Chem. 70 (1998) 4286.
[20] S. Jadhav, E. Bakker, Anal. Chem. 71 (1999) 3657.
[21] S. Jadhav, A.J. Meir, E. Bakker, Electroanalysis 12 (2000) 1251.
[22] S. Jadhav, E. Bakker, Anal. Chem. 73 (2001) 80.
[23] A. Shvarev, E. Bakker, Anal. Chem. 75 (2003) 4541.
[24] A. Shvarev, E. Bakker, J. Am. Chem. Soc. 125 (2003) 11192.
[25] Z. Samec, V. Marecek, J. Koryta, M.W. Khalil, J. Electroanal. Chem. 83 (1977) 393.
[26] J. Koryta, Electrochim. Acta 24 (1979) 293.
[27] V. Marecek, Z. Samec, J. Koryta, Adv. Colloid Inter. Sci. 29 (1988) 1.
[28] P. Vanysek, Electrochemistry on Liquid/Liquid Interfaces, Springer, Berlin, 1985.
[29] O. Shirai, S. Kihara, Y. Yoshida, M. Matsui, J. Electroanal. Chem. 389 (1995) 61.
[30] M. Senda, T. Kakiuchi, T. Osakai, Electrochim. Acta 36 (1991) 253.

[31] W.E. Morf, The Principles of Ion-Selective Electrodes and of Membrane Transport, Elsevier, New York, 1981.
[32] W.E. Morf, M. Badertscher, T. Zwickl, N.F. de Rooij, E. Pretsch, J. Phys. Chem. B 103 (1999) 11346.
[33] T. Kakiuchi, Electrochim. Acta 44 (1988) 171.
[34] T. Zwickl, PhD Thesis, ETH Zürich, Nr. 15485, 2004.
[35] J. Langmaier, K. Stejskalová, Z. Samec, J. Electroanal. Chem. 496 (2001) 143.
[36] S.M. Ulmeanu, H. Jensen, Z. Samec, G. Bouchard, P.A. Carrupt, H.H. Girault, J. Electroanal. Chem. 530 (2002) 10.
[37] U. Oesch, W. Simon, Anal. Chem. 52 (1980) 692.
[38] M.L. Iglehart, R.P. Buck, G. Horvai, E. Pungor, Anal. Chem. 60 (1988) 1018.
[39] B.D. Pendley, R.E. Gyurcsányi, R.P. Buck, E. Lindner, Anal. Chem. 73 (2001) 4599.
[40] M. Püntener, M. Fibbioli, E. Bakker, E. Pretsch, Electroanalysis 14 (2002) 1329.
[41] W.E. Morf, T. Zwickl, E. Pretsch, N.F. de Rooij, Chimia (2003) 639.
[42] T. Sarada, L.C. Sawyer, M.I. Ostler, J. Membr. Sci. 15 (1983) 97.
[43] T. Sokalski, T. Zwickl, E. Bakker, E. Pretsch, Anal. Chem. 71 (1999) 1204.
[44] A. Ceresa, T. Sokalski, E. Pretsch, J. Electroanal. Chem. 501 (2001) 70.
[45] Y. Marcus, Ion Properties, Marcel Dekker, New York, 1997.